View metadata, citation and similar papers at core.ac.uk
brought to you by CORE
provided by Woods Hole Open Access Server

Rapid lateral particle transport in the Argentine Basin: Molecular ^{14}C and $^{230}Th_{xs}$ evidence

Gesine Mollenhauer[1,2,*], Jerry F. McManus[1], Albert Benthien[1,2], Peter J. Müller[3] & Timothy I. Eglinton[1]

[1]Woods Hole Oceanographic Institution
[2]now at: Alfred-Wegener-Institute for Polar and Marine Research
[3] Universität Bremen, Fachbereich Geowissenschaften
[*]to whom correspondence should be addressed; gmollenhauer@uni-bremen.de

Abstract

Recent studies have revealed that lateral transport and focusing of particles strongly influences the depositional patterns of organic matter in marine sediments. Transport can occur in the water column prior to initial deposition or following sediment re-suspension. In both cases, fine-grained particles and organic-rich aggregates are more susceptible to lateral transport than coarse-grained particles (e.g. foraminiferal tests) because of the slower sinking velocities of the former. This may lead to spatial and, in the case of redistribution of re-suspended sediments, temporal decoupling of organic matter from coarser sediment constituents. Prior studies from the Argentine Basin have yielded evidence that suspended particles are displaced significant distances (100 - 1000 km) northward and downslope by strong surface and/or bottom currents. These transport processes result in anomalously cold alkenone-derived sea surface temperature (SST) estimates (up to 6°C colder than measured SST) and in the presence of frustules of Antarctic diatom species in surface sediments from

this area. Here we examine advective transport processes through combined measurements of compound-specific radiocarbon ages of marine phytoplankton derived biomarkers (alkenones) from core-tops and excess ^{230}Th ($^{230}Th_{xs}$)-derived focusing factors for late Holocene sediments from the Argentine Basin. On the continental slope, we observe $^{230}Th_{xs}$-based focusing factors of 1.4 to 3.2 at sites where alkenone-based SST estimates were 4 – 6 °C colder than measured values. In contrast, alkenone radiocarbon data suggest coeval deposition of marine biomarkers and planktic foraminifera, as alkenones in core-tops were younger than, or similar in age to, foraminifera. We therefore infer that the transport processes leading to the lateral displacement of these sediment components are rapid, and hence probably occur in the upper water column (< 1500 m).

Keywords: Sediment transport; radiocarbon dating; $^{230}Th_{xs}$; $U^{K'}_{37}$ sea-surface temperatures; core-top sediments; South Atlantic Ocean; Argentine and Brazil Basins; Brazil-Malvinas Confluence

Introduction

The value of deep-sea sediments as records of climate history has long been recognized. Past environmental conditions of the oceans can be reconstructed from physical and chemical characteristics of sediment constituents, so-called proxy parameters. The carriers of the various proxies can reside in different grain-size fractions and are associated with different types of sedimentary constituents (e.g. biogenic carbonates, organic matter, and lithic grains such as clay particles).

It is well known that post-depositional processes (e.g. diagenesis or bioturbation) can affect the fidelity of sedimentary records and thereby reduce their potential for accurately recording past climate conditions (e.g. Guinasso & Schink, 1975; Bard et al., 1987; Thomson et al., 1995; Hedges et al., 1999; Bard, 2001). Pre-depositional lateral transport of particles

within the water column is an additional process that potentially can affect the paleoceanographic record (e.g. Thomsen et al., 1998; Santschi et al., 1999; Freudenthal et al., 2001). Displacement of particles from their point of origin reduces our ability to accurately reconstruct past environmental conditions at a given location. Furthermore, lateral transport has the potential to sort sediment particles hydrodynamically according to size and sinking velocity and may thus result in decoupling of proxy records residing within different particle classes. These processes remain poorly understood but have recently been the subject of increased attention and debate (e.g., Marcantonio et al., 2001).

Two separate approaches have been taken to investigate sediment transport and its effect on paleoceanographic records. The first employs uranium (U)-series isotopes to understand and quantify lateral particle transport in the oceans (Suman & Bacon, 1989; Thomson et al., 1999; Marcantonio et al., 2001; François et al., 2004; Loubere et al., 2004). This method relies upon an essentially constant amount of dissolved uranium in seawater coupled with highly particle reactive daughter isotopes (primarily Thorium-230 (^{230}Th) and Protactinium-231 (^{231}Pa)). The estimated vertical component of sediment flux is based on the assumption of rapid scavenging of ^{230}Th by sinking particles. It is assumed that at any given time and location the production of ^{230}Th in the water column is known and equal to the rate of decay of ^{234}U, and that the mode of ^{230}Th scavenging into the sediment by adsorption of this isotope is also well-known and constant with time (for details see: François et al., 2004). Preserved vertical fluxes of sediments are calculated by normalizing to the decay-corrected concentration of ^{230}Th in sediments as a function of water depth.

Estimates of sediment focusing can be based on the assumption that the scavenged ^{230}Th inventory of the sediment between two given depths matches the production in the overlying water column integrated over the time of accumulation of this depth interval. If the inventory is bigger than expected, it is concluded that the sediments are focused. Focusing is quantified by a focusing factor (Ψ), which is calculated as the ratio of the inventory and the production

over the time of accumulation. Thus, Ψ values greater than unity indicate focusing, while Ψ values less than 1 imply the occurrence of sediment winnowing. Using this approach, several authors have argued that observed sediment accumulation maxima (e.g. in the equatorial Pacific) formerly interpreted as paleoproductivity signals (Paytan et al., 1996) are instead a consequence of changes in lateral particle supply (Marcantonio et al., 2001; Loubere et al., 2004), although this interpretation is the subject of intense debate.

Potential temporal decoupling of organic and inorganic proxies, associated with the fine and coarse sediment fractions, respectively, resulting from lateral sediment transport has also been investigated by molecular-level radiocarbon dating (Ohkouchi et al., 2002; Mollenhauer et al., 2003, 2005). Significant age offsets between a suite of marine organic biomarkers (alkenones) associated with the fine fraction and coarse grained calcareous foraminiferal tests have been found at sites of high local sedimentation rates. Age offsets of up to 8 kyr occur at the Bermuda Rise, a well described sediment drift, and have been attributed to the advection of fine-grained sediment from the Canadian continental margin (cf. Keigwin & Jones, 1994; Ohkouchi et al., 2002). Significant age differences between organic matter and foraminifera have also been reported from continental margins where high sedimentation rates are observed in local depo-centers (Mollenhauer et al., 2003, 2005). Other studies have found independent evidence of lateral displacement of fine-grained particles based on sedimentological considerations (Thomsen et al., 1998; Benthien & Müller, 2000; Freudenthal et al., 2001; Englebrecht & Sachs, 2005).

The Argentine Basin represents a good example of an oceanic area affected by large-scale sediment advection. Several studies have suggested that extensive northward displacement of fine-grained particles and phytoplankton detritus occurs in this region. For example, core-top sediment characteristics such as diatom floral assemblages (Romero & Hensen, 2002) and reconstructed sea-surface temperatures (SST) based on the alkenone-derived $U^{K'}_{37}$ index (Brassell et al., 1986; Prahl et al., 1988; Müller et al. 1998) are

inconsistent with overlying surface water conditions (Benthien & Müller, 2000; Figure 1c). These observations are interpreted as being the result of particle advection via surface currents containing colder, Antarctic waters, or from cooler coastal areas via bottom current transport. Conte et al. (2006) report cold anomalies in SST estimates derived from alkenones in surface waters of the Argentine Basin, arguing for long-range transport via surface currents.

The study area (Figure 1a) is situated in the southwestern Atlantic Ocean ranging from approximately 35°W to 60°W and from 20°S to 45° S. Bathymetrically, this area is divided into the Brazil Basin in the north and the Argentine Basin in the south, both with maximum depths over 5000 m. The two basins are separated by the Rio Grande Rise and the Santos Plateau. The Vema Channel, a narrow (20 km wide) incision at 4620 m depth allowing for deep water to propagate from the south into the Brazil Basin, separates the Rio Grande Rise from the Santos Plateau and the continental slope.

The upper-level circulation pattern in the study area (Figure 1b) is dominated by the southward-flowing Brazil Current and the northward-directed Malvinas Current, both flowing along the continental margin (Peterson & Stramma, 1991). The warm-water Brazil Current originates near 10°S, where the South Equatorial Current bifurcates. It is a weak western boundary current carrying warm and salty subtropical water masses with surface velocities between 20 and 60 cm s^{-1}. The flow strengthens at more southern latitudes under the influence of a recirculation cell (Peterson & Stramma, 1991). The Malvinas Current originates east of the Drake Passage as a branch of the Antarctic Circumpolar Current (Peterson, 1992). It transports cold and less saline subantarctic waters and encounters the Brazil Current near 38°S, an area referred to as the Brazil-Malvinas Confluence. There both currents separate from the continental margin and flow seaward in a south-eastward direction. In the confluence zone, strong thermal gradients in surface waters are observed, often reaching 1°C km^{-1} (Olson et al., 1988). Direct measurements of current velocities in the Malvinas Current are scarce. Drifter experiments revealed a northward core flow velocity of 60 – 80 cm s^{-1} (Peterson et al.,

1996). Highest velocities of up to 100 cm s^{-1} in the Malvinas Current region were observed in the southward Brazil-Malvinas Return flow, whose flow path is offshore from the boundary currents (Peterson et al., 1996; Piola et al., http://www.po.gso.uri.edu/wbc/Piola/bmc.htm).

At the Brazil-Malvinas Confluence, the lower-level circulation is also characterized by the interplay between several water masses (e.g. Reid et al., 1977). The subtropical water masses of the Brazil Current and the subantarctic waters of the Malvinas Current meet in the upper 800 m of the water column. Antarctic Intermediate Water is detected between 500 and 1500 m. Bottom currents underlying the Malvinas Current between 400 and 1600 m depth range between 20 and 30 cm s^{-1} (Peterson et al., 1996). North Atlantic Deep Water (NADW) is found at around 2500 m water depth and flows southward along the continental rise until it turns eastward at around 38° S (Maamaatuaiahutapu et al., 1992). Flow velocities in the NADW depth range are less than 5 cm s^{-1} (Hogg et al., 1996). Northward flowing Circumpolar Deep Water is separated by NADW into an upper and a lower branch. At depth, Weddell Sea Deep Water, as part of Antarctic Bottom Water (AABW), flows northward near the bottom of the Argentine Basin (Peterson, 1992). While most currents below 800 m depth are relatively sluggish (<5 cm s^{-1}), flow of AABW through the Vema Channel can reach velocities up to 25 cm s^{-1} (Hogg et al., 1996). The Vema Channel thus is the major conduit for AABW to propagate northward into the Brazil Basin, with transport of up to 4 Sv (Hogg et al. 1999).

Productivity in the study area is highest along the continental margin of the Argentine Basin, in particular off the mouth of the Rio de la Plata (Figure 1b). Satellite imagery clearly shows the frequent occurrence of eddies spinning off the Brazil-Malvinas Confluence zone. To the south of the confluence zone, nutrient-richer Malvinas Current waters are thus transported offshore. As a result, average annual pigment concentration is higher in the Argentine Basin than in the oligotrophic Brazil Basin (Antoine et al., 1996). Sources of marine particulate organic carbon are therefore larger in the south and west of the study area

than in the north and east. This pattern is also reflected in the organic carbon contents of the sediments (see below; Figure 1d). Possible sources of laterally advected sediments are the shelf areas as described by Michaelovitch de Mahiques et al. (2002) for the Brazil Basin. According to Benthien & Müller (2000), suspended particles can also be advected from the south over distances of up to 1000 km. In addition, strong and dominantly northward directed bottom currents prevailing in the Argentine Basin can lead to sediment remobilization and redistribution. High kinetic energy related to the Brazil-Malvinas Confluence may induce benthic storms resulting in extensive reworking and sediment redistribution (cf. Hollister & McCave, 1984).

Deep-sea sediments in this region are dominated by carbonates and, below approximately 4000 m water depth, by clays. Input of terrigenous material through the Rio de la Plata is approximately 92 Gt annually (Milliman & Meade, 1983), including significant amounts of terrigenous organic matter (Schlünz et al., 1999, Seiter et al., 2004). Organic carbon concentrations in central basin surface sediments are generally low (<0.5 % dry weight), but a local maximum reaching values of up to 2 % exists on the continental slope underlying the Malvinas-Brazil Confluence Zone (Figure 1d; Mollenhauer et al., 2004; Seiter et al., 2004)

In the present paper, we report the first coupled U-series and molecular ^{14}C-based study of sediment supply and deposition. We use U-series isotopes to assess sediment focusing in selected core-top sediments from the Argentine and Brazil Basins. Areas apparently unaffected by northward sediment advection were considered as well as those where the largest anomalies have been reported (Benthien & Müller, 2000; Romero & Hensen, 2002). In addition, we studied radiocarbon ages of coarse-grained foraminifera, total organic carbon (TOC) and alkenones in the same sediment samples. We show that although the ^{230}Th-based focusing factor (Ψ) data imply the occurrence of sediment focusing in areas with large temperature anomalies, molecular-level radiocarbon analyses do not yield a clear transport

signal. We use the data, together with evidence from the literature (Lange, 1985; Conte et al., 2006), to infer that long-range lateral transport of phytoplankton detritus over several hundred kilometres can occur during, or shortly after production in surface waters.

Samples

We used multicorer sediment samples taken from 10 sites on the continental margin and in the deep Argentine and Brazil Basins. Out of those sites, 8 have been discussed in the study of Benthien & Müller (2000). Two new sites located near previously studied locations were added (Figure 1c, Table 1). From each site, we used core-top or near-surface (0-1, 0-2 or 1-2 cm) samples for radiocarbon dating of foraminifera, TOC and alkenones (Table 2). Additional foraminiferal radiocarbon dates were obtained from samples taken from the bottom (i.e. sediment depths of between 10 and 40 cm) of one multicorer subcore at each site (see Table 2 for precise sample depths). Uranium-series isotope analyses were also performed on subsamples from multi-core tops and bottoms at each site.

Methods

Radiocarbon analyses

Accelerator mass spectrometer (AMS) radiocarbon ages were determined on TOC and planktic foraminifera for each of the 10 core-top samples. Where abundances were sufficient, molecular-level radiocarbon dates of C_{37}, C_{38} and C_{39} alkenones (measured as a composite sample) were also obtained. All radiocarbon measurements were performed at the National Ocean Sciences Accelerator Mass Spectrometry (NOSAMS) facility at the Woods Hole Oceanographic Institution, USA, following standard procedures for TOC and foraminifera (McNichol et al., 1994). Briefly, subsamples of homogenized bulk sediments containing approximately 1 mg of organic carbon were hydrolyzed with 10% hydrochloric acid and combusted in evacuated, pre-combusted quartz tubes with copper oxide and silver. Resulting

CO_2 was purified and graphitized over an iron catalyst; graphite targets were then pressed for AMS analysis. Planktic foraminifera were picked from the >125 µm (>150 µm for GeoB6201, GeoB6339 and GeoB2734) fraction of wet-sieved subsamples or solvent-extracted sediment residues (GeoB6201, GeoB6339 and GeoB2734). For each sample, the most abundant shallow-dwelling species was chosen (Table 2). Mixed planktic species were picked in carbonate-poor samples (Table 2). In addition to wet-sieving, samples were ultrasonically cleaned in Milli-Q water if visual inspection suggested the presence of contamination. Foraminiferal shells were dissolved by standard procedures (McNichol et al., 1994). The resulting gas was purified, converted to graphite and analysed by AMS by procedures identical to those used for TOC.

Alkenone samples were purified from total lipid extracts of 100-200 g of freeze-dried homogenized sediments by the methods of Ohkouchi et al. (2005). A sequence of wet-chemical techniques including saponification, silica-gel chromatography, urea adduction and silver nitrate/silica gel chromatography was employed. Yields and sample purities were checked with a gas chromatograph equipped with a flame ionization detector (GC/FID). Purified samples consisted of C_{37}, C_{38} and C_{39} alkenones and were quantified with behenic acid myristyl ester as an external standard. Pure alkenone samples were subsequently sealed with copper oxide in pre-combusted evacuated quartz tubes and combusted at 850°C. Resulting CO_2 gas was purified, quantified and converted to graphite with cobalt as a catalyst for radiocarbon analysis by AMS. Alkenone samples yielded 37-220 µg carbon and were analysed by dedicated techniques for small samples (Pearson et al., 1998).

Radiocarbon ages are reported as conventional radiocarbon ages (Stuiver & Polach, 1977). This notation involves a correction for isotope fractionation occurring during sample formation or processing; i.e., all data are normalized to a $\delta^{13}C$ value of -25‰. In this way, carbonate and organic matter samples can be compared. For the purposes of assessing the age relationships in core-top samples, no conversion to calendar ages is necessary. In order to

derive a best estimate of depositional age of the sediments, foraminiferal ages were, however, converted to calendar ages with the calibration software CALIB 5 (Stuiver & Reimer, 2005). Sedimentation rates can be calculated by linear interpolation between these calibrated ages of core-top and bottom intervals. Information on sediment mixed-layer depths at the core sites is not available.

Uranium-series analyses

For U-series isotope analyses, 0.3 to 0.4 mg of dried and homogenized sediment samples were spiked with ^{229}Th and dissolved by acid digestion in HNO_3, $HClO_4$ and HF. In addition to unprocessed freeze-dried and homogenized samples, we studied organic solvent extracted sediment residues from four core sites as well. The acid digested samples were processed by a procedure for separation of Th fractions by anion exchange described by Choi et al. (2001). U-series isotopes were extracted from the acid digested samples by iron oxy-hydroxide (FeOOH) co-precipication (3 times), where FeOOH was recovered by centrifugation and decantation. Iron oxy-hydroxides and co-precipitates were re-dissolved in 9 N HCl by adding a volume of concentrated HCl (12 N) equivalent to three times the volume of FeOOH. After small aliquots for determination of the ^{238}U/^{232}Th ratio were taken, the samples were passed through a ~4 ml column packed with AG1-X8 resin and preconditioned with 9 N HCl. Th was eluted with an additional 12 ml of 9 N HCl, the eluate being collected in a Teflon beaker. The Th fraction was then evaporated to a small volume, taken up in 8 N HNO_3 and further purified by elution through a second anion exchange column of AG1-X8, this time pre-conditioned with 8 N HNO_3. After elution, the Th fraction was reduced by evaporation to a drop in a small screw-cap Teflon vial. Just prior to analysis by inductively coupled plasma mass spectrometry (ICP/MS), 0.3 ml of Milli-Q water was added.

The concentrations of ^{230}Th were calculated from the ^{230}Th/^{229}Th ratio with a magnetic sector ICP/MS (Finnigan MAT Element) (for method details see Choi et al., 2001).

Background corrections were based on analysis of method and column blanks. Excess ^{230}Th ($^{230}Th_{xs}$) corrected for contribution of ^{230}Th derived from decay of detrital ^{238}U was estimated from the measured concentration of ^{232}Th in the sediment and an assumed average activity ratio of detrital ^{238}U and ^{232}Th of R=0.6 (McManus et al., 1998; Henderson & Anderson, 2003). A correction for radiocarbon decay of the unsupported ^{230}Th with a halflife of 75.7 kyr is made based on the calibrated foraminiferal radiocarbon ages (François et al., 2004; Table 3). Ingrown ^{230}Th from decay of authigenic ^{234}U is estimated from an assumed activity ratio of ^{234}U and ^{238}U of 1.14 and from the decay formula and the measured radiocarbon sediment age. The resulting corrected value $^{230}Th_{xs0}$ is then used for calculation of focusing factors and sediment fluxes, employing the equations given in François et al. (2004). Where core-top and core-bottom values were significantly different, duplicate runs were performed (GeoB2116).

It should be noted that estimation of focusing factors relies on the knowledge of dry bulk density of the sediment for the calculation of the inventory, and on accurate age data for the interval over which the focusing factors are calculated. Moreover, focusing factors are averages over sediment intervals and cannot be derived at a higher resolution than the available age tie points.

In this study, we used measured dry bulk density (DBD) values for most of the core-top sediments (Müller, unpublished data). Where no data were available for core-top sediments, values derived from comparison with neighboring cores were assumed. DBD used for core bottoms were an assumed average value of 0.7 g/cm³ (0.9 g/cm³ for GeoB6339, where the assumed core-top value was 0.7 already), which is the mean DBD for sediments in the upper half meter of gravity cores taken from the Brazil and Argentine Basin margins (Müller, unpublished data). Focusing factors were furthermore calculated from the mean of core-top and –bottom $^{230}Th_{xs0}$ and the calibrated radiocarbon ages of foraminifera from the respective core slices. Where no foraminiferal dates were available, assumed ages were based on sedimentation rates observed in the vicinity of the core sites.

Results and Discussion

Core-top radiocarbon ages of foraminifera, TOC and alkenones, $^{230}Th_{xs}$ normalized fluxes and sediment focusing factors based on $^{230}Th_{xs}$ are given in Table 2 and 3 and shown on Figures 2, 3 and 4. Despite compelling evidence for lateral transport as an important influence on the sedimentation in the Argentine Basin, in particular on the sedimentation of alkenones (Benthien & Müller, 2000), our data based on organic matter radiocarbon ages do not immediately imply sediment redistribution. Specifically, alkenones in core-top sediments are either the youngest dated sediment constituent or less than 300 years older than co-occurring foraminifera. $^{230}Th_{xs}$ inventories on the continental margin of the Argentine Basin imply sediment focusing at sites with reported large negative deviations from measured sea-surface temperatures (SST) in reconstructed SSTs based on alkenone $U^{K'}_{37}$ (ΔT), but they are not systematically higher in all of the areas with large reported ΔT (i.e., in the Vema Channel). Here we will first discuss core-top radiocarbon ages, followed by a discussion of the $^{230}Th_{xs}$ based data.

Core-top radiocarbon ages

In most cases, we regard foraminiferal radiocarbon ages as the most reliable source of information on the time of deposition of the sediment. This is because foraminifera are part of the sand grain size fraction, whereas organic matter is associated with fine-grained and low-density material (Suman & Bacon, 1989; Keigwin & Schlegel, 2002). Foraminifera larger than 125 μm can be assumed to fall vertically through the water column and are not easily re-distributed (Fok-Pun & Komar, 1983). In contrast, organic matter may be incorporated into nepheloid aggregates once it reaches the dynamic and high shear nepheloid layer depths, where frequent resuspension leads to offshore transport and dispersion (Ransom et al., 1998).

"Old" core-top radiocarbon ages of TOC (2000 – 3500 ^{14}C years) or offsets between radiocarbon ages of planktic foraminifera and TOC (up to 7000 ^{14}C years) , where foraminifera are younger, have been reported from many settings (e.g. Hall & McCave, 1998; Bauer et al., 2001; Ohkouchi et al., 2002, Mollenhauer et al., 2003; Keil et al., 2004). They have been explained by input of pre-aged terrigenous organic matter, advection of re-suspended organic material or a combination of the two. Alkenones exclusively represent phytoplankton organic matter derived from marine surface waters. Therefore, alkenones that are older than co-occurring foraminifera can reliably be attributed to advective supply of "pre-aged" material or aging of phytoplankton detritus in continuous loops of re-suspension and re-sedimentation during lateral transport (Ohkouchi et al., 2002; Mollenhauer et al., 2003). In core-top sediments, organic matter older than foraminifera may also be explained by differential bioturbation (Bard, 2001), in which old fine-grained organic matter is preferentially mixed upward from deeper sediment layers, resulting in an older mixed-layer age for fine-grained than for coarse-grained particles. This effect is expected to be strongest at sites with sedimentation rates less than 10 cm/kyr (e.g. Anderson, 2001; Bard, 2001).

Age offsets between organic matter and foraminifera in the opposite sense are more difficult to interpret. If down-core foraminiferal abundances were highly variable and very low at present, then core-top radiocarbon ages could potentially be biased towards older ages due to mixing (Broecker et al., 1999). If organic matter flux were at the same time less variable or even increased at present, those foraminiferal core-top ages could be older than TOC ages. Alternatively, foraminifera older than TOC could result from winnowing, exposing "relict" foraminifera followed by a shorter phase of undisturbed deposition of coarse and fine-grained sediment, or from lateral supply of eroded coarse-grained relict sediments to the core site.

The studied core-sites can be grouped geographically: the Brazil Basin, the Vema Channel and the Argentine Basin. Core top radiocarbon ages of all dated sediment

constituents display a large variability in all basins and range from modern (i.e. containing bomb-radiocarbon) to close to 8000 radiocarbon years (Figure 2). Despite this large variability in age, these data rule out the possibility that any deviations in the reconstructed SSTs from measured values (ΔT) as reported by Benthien & Müller (2000) are caused by analysis of glacial sediments at sites without Holocene sedimentation.

Core-top samples from the Argentine Basin in the area with highest alkenone SST ΔT uniformly display foraminiferal ages of less than 2000 years (modern, 410±25 ^{14}C years, 1930±30 ^{14}C years). Modern core-top foraminifera were found at sites GeoB2804 and GeoB2805 for which ΔT values of -5.1° and -4.5° C respectively were reported. At the three of the four sites from the Argentine Basin where foraminifera were sufficiently abundant for radiocarbon analyses, TOC in core-tops is 1320, 1300 and 1620 radiocarbon years older than the corresponding foraminifera. Considering the relatively high sedimentation rates (5 to 14 cm/kyr) and the location of these sites on the continental margin and near the Rio de la Plata mouth, the older TOC in core-top sediments may be attributed to inputs of "pre-aged" and possibly terrigenous organic matter. This is corroborated by the two alkenone core-top ages from the Argentine Basin. Alkenone samples are 920±185 and 1340±105 radiocarbon years younger than the respective TOC. At site GeoB2734, alkenones and foraminifera ages differ by less than 300 years, while at site GeoB6339 alkenones are even younger than co-occurring foraminifera. The young alkenones in core-tops indicate that they were rapidly deposited, and good agreement with foraminifera suggests that both components derive from overlying surface waters, implying a different, potentially non-marine source of organic carbon contributing to older TOC ages.

In the Vema Channel area, high ΔT values of -3.9 and -4.7°C have been reported at sites below ca. 3950 m and attributed to lateral transport of alkenones by Lower Circumpolar Deep Water (Benthien & Müller, 2000). At one of these deep sites, GeoB2826, we observe old core-top ages of 4450 and 4920 radiocarbon years for foraminifera and bulk organic matter,

respectively, while at the deepest site, GeoB2824, carbonate dissolution allowed only TOC to be dated. The latter was found to be 2400 ^{14}C years old. The old ages at GeoB2826 may be the result of very low sedimentation rates combined with bioturbation. Sedimentation rates at this site are estimated to range between 0.7 and 1.5 cm/kyr, based on the foraminiferal radiocarbon ages of the core-top and -bottom samples (the low value is calculated if the core-top is assumed to be modern, the higher value results from linear interpolation of the dated radiocarbon ages of the core-top and –bottom). If these old core-top radiocarbon ages are caused by bioturbation leading to homogenization of the uppermost sediment, sedimentation rates calculated from ages of foraminifera in near-surface sediments will underestimate the true sedimentation rate. Interpolation between an assumed modern core-top age and an age from below the mixed layer would in this case yield a more realistic estimate of sedimentation rate, illustrating the range of possible values. Alternatively, old foraminifera and TOC in core-top sediments could be explained by erosion of more recent sediment in this area, which is characterized by strong bottom currents.

In the Brazil Basin, where reconstructed sea-surface temperatures agree well with measured values, core-top radiocarbon ages are difficult to explain. At two of the three Brazil Basin sites studied here, foraminifera are significantly older than TOC, and also older than alkenones at site GeoB6201. These two sites are at a very shallow (473 m, GeoB6201) and a very deep (4164 m, GeoB2116) location. The latter site is at a water depth where calcite preservation is poor, which may in part explain the observed high foraminiferal core-top age of 7370 ^{14}C years. However, TOC is also very old at this site (5080 ^{14}C years). One possible explanation for the age structure is that this abyssal site is influenced by downslope transport, possibly a turbidity flow. Alternatively, the “old” core-top ages could reflect very low Holocene sedimentation rates (see below).

Site GeoB6201, in contrast, is located close to the coast. Similar core-top and –bottom radiocarbon ages of foraminifera (3240±35 and 3660±30 ^{14}C years, respectively) imply

intense bioturbation as is common in slope sediments. However, TOC and alkenones at GeoB6201 are significantly (1000 and 1300 ^{14}C years) younger than co-occurring foraminifera. Bioturbation therefore may not be the main control on the core-top ages at this site, as organic matter would be expected to be more intensely mixed and homogenized to deeper depths, and as a result would appear older than foraminifera in surface sediments. Moreover, sediment surface TOC contents of ~0.6 % do not imply an environment of intense bioturbation. The shallow-water setting renders the core site susceptible to re-working processes. Indeed, the preservation state of the foraminifera seems to indicate that re-working has occurred, as the tests were visibly corroded. Re-working of shelf sediments is also implied by very heterogeneous radiocarbon ages of carbonate in very shallow (40 - 90 m) shelf sediments near 19 °S (Table 4; J. Pätzold & H. Arz, unpublished data).

The northernmost site of this study is GeoB2124, where core-top sediment ages of 655±30 ^{14}C years for forams and 1370±65 ^{14}C years for TOC suggest deposition of marine material with only moderate bioturbational mixing. Input of pre-aged terrigenous organic matter resulting in a slightly greater TOC core-top age is also likely. Carbonate core-top ages of 565±30, 970±30 and 2050±20 ^{14}C years are observed at other intermediate depth sites in the Brazil Basin (2000 – 2500 m) (Table 4; Arz et al., 2001; Dürkoop, 1998; Mollenhauer, 1999).

Notably, the core-top radiocarbon ages of planktic foraminifera are youngest at water depths between approximately 1800 and 2800 m (Figure 3). This depth range corresponds to the flow path of NADW (Mémery et al., 2000), which is less corrosive to carbonate than the southern sourced water masses. Similar distributions of foraminiferal core-top ages, i.e. older ages in more corrosive waters, have been reported by Broecker et al. (1991). These authors, however, have not offered a steady-state explanation for this observation. Better carbonate preservation as a function of lesser water mass corrosiveness in these water depths of the

Argentine continental margin have also been inferred from carbonate contents of surface sediments (Frenz et al., 2003).

$^{230}Th_{xs}$-derived focusing factors (Ψ)

Sediment fluxes and focusing factors are listed in Table 3 and summarized in Figures 3 and 4. Focusing values generally encompass intervals spanning several hundred to up to 6 thousand years during the Holocene, with the exception of two Brazil Basin cores, where Ψ are calculated over longer time intervals (Table 3). In the Argentine Basin, all sites have enriched $^{230}Th_{xs}$ inventories with Ψ>1. At the deepest site GeoB2728 in 4643 m water depth, because of the lack of preserved foraminifera, there is no absolute age control at this point, and the focusing factor of 1.4 is based on an age estimate using an assumed sedimentation rate of approximately 3 cm/kyr (Mollenhauer et al., 2004). If the sedimentation rate is assumed to be less than 2 cm/kyr, Ψ would be <1, and Ψ values >2 are calculated at assumed sedimentation rates of ~4.5 cm/kyr. This exercise illustrates the sensitivity of calculated Ψ to uncertainties in sedimentation rates. Therefore, the calculated focusing factor at site GeoB2728 carries great uncertainty and cannot be used to make strong statements.

At sites GeoB2804, GeoB2805 and GeoB2734, which are located within the area with the highest observed ΔT values, $^{230}Th_{xs}$ inventories clearly indicate sediment focusing (Ψ =3.0, 1.4 and 2.1, at 1836 m, 2743 m and 2295 m respectively). This distribution may reflect a typical continental slope pattern, where a depo-center exists at intermediate slope depths. However, probably because of the strong bottom currents between 400 and 1600 m water depth (Peterson et al., 1996), it seems to be at a greater depth than on other continental slopes, where typical depo-center depths range between 500 and 1500 m water depth (e.g. Anderson et al., 1994; Buscail et al., 1997; Sanchez-Cabeza et al., 1999; Martin & Sayles, 2004). It is worth noting that downslope transport leading to the development of a mid-slope depo-center

will be underestimated when the $^{230}Th_{xs}$ method is used, owing to the assumptions made when focusing factors are calculated (François et al., 2004).

Sediment focusing at intermediate slope depths is also indicated by a focusing factor of 3.2 calculated for site GeoB6339 (2492 m; Figures 3 & 4). The sample sites are located within the depth range of NADW influence, whose more sluggish current velocities may favor deposition of fine-grained material. GeoB6339, however, is located further south than the range of NADW. Thus, the generally higher focusing factors are probably not related to a specific water-mass.

Our results compare favorably with published results from other continental margins. Thomson et al. (1999) calculated focusing factors for sediment cores retrieved from the Iberian Margin at water depths of 2465 and 3381 m. Their data imply sediment focusing by factors of 4 and 3.2 over a 140 kyr interval, and Holocene values of 4 and 2.7, respectively. Ψ values between 0.5 and 2.2 have also been found at 2500 to 2600 m water depth on the Ontong Java Plateau (Schwarz et al., 1996; Higgins et al., 2002), while sediment focusing by factors of 1-8 have been reported for cores from between 2700 and 3900 m water depth in the Equatorial Pacific (Loubere et al., 2004; Kienast et al., manuscript in preparation).

Estimates of $^{230}Th_{xs}$ inventories at the two core sites from the Vema Channel (Ψ ~0.9) may suggest the occurrence of sediment winnowing as a result of strong bottom currents (up to 25 cm s^{-1}) prevailing in this area. It should be noted, however, that the focusing factor calculated for site GeoB2824 is based on a crude age estimate, as sufficient foraminifera were not available for radiocarbon dating of the sediment. Here, we assumed a sedimentation rate of approximately 1.5 cm/kyr (approximately the rate observed at the neighboring core site GeoB2826). Normalized fluxes were also low at these two sites. Assuming this sedimentation rate, which is considered an upper limit of possible values, yields an estimate of a maximum value for sediment focusing. Furthermore, the calculated Ψ values of 0.9 are not significantly different from 1, which makes the evidence for the occurrence of winnowing in the Vema

Channel very weak. However, together with the reported high current velocities through the Vema Channel (Hogg et al., 1996, 1999), we regard the observed low Ψ at site GeoB2826 as an indication for the general occurrence of winnowing in the area.

In the Brazil Basin, the $^{230}Th_{xs}$ inventory at site GeoB2124, located at intermediate water depth on the continental slope and bathed by NADW, does not imply the presence of a depo-center. Instead, sediment winnowing seems to be operative at this location (Ψ = 0.8). This interpretation contrasts with that from grain-size distribution data, where no evidence for winnowing has been found on the Brazil Basin continental margin (Frenz et al., 2003).

Calculated Ψ implies the occurrence of focusing at the deep site GeoB2116 (Ψ =1.7), although significantly different $^{230}Th_{xs0}$ concentrations in core-top and –bottom samples were observed here. The latter implies that the assumption of homogeneous sedimentation over the sediment interval covered by the multi-core, which is generally made when in the calculation of Ψ from an averaged $^{230}Th_{xs0}$ concentration of core-top and –bottom sediment, may not be valid at this site. Radiocarbon ages place the core-top in the early to mid-Holocene (7.8 kyr), while the core-bottom is glacial (19.5 kyr). Different sedimentation regimes may have prevailed during the glacial than during the Holocene, a notion corroborated by the flux data (Table 3). If we assume that the core-top $^{230}Th_{xs0}$ value is representative for the Holocene, and the core-bottom value is representative for the glacial, we can calculate possible scenarios for Holocene and glacial sediment focusing or winnowing: 1) If sedimentation rates were constant, there would be stronger sediment focusing in the Holocene than in the glacial. 2) If sedimentation rates were very low in the Holocene (1cm/kyr) and higher during the glacial (~3.9 cm/kyr), focusing would be implied (Ψ=2.2) during the glacial, while the Holocene value would represent slight winnowing (Ψ=0.7). 3) Constant slight focusing (Ψ=1.7) throughout the entire interval could have occurred if sedimentation rates were ~2.5 cm/kyr and ~3.6 cm/kyr in the Holocene and glacial respectively.

The GeoB2116 core site is located north of the Vema Channel, which makes it a likely location of sediment focusing. Material suspended by bottom currents passing through the deep throughflow with higher velocities is likely re-deposited after passage through the Vema Channel in an area of slackening current velocities. However, modern current trajectories of deep water flowing northward through the Vema Channel are directed slightly to the west (Hogg et al., 1996), while site GeoB2116 is located to the north and east of the Vema Channel. It is therefore not known at this point whether the material entrained in the through-flow water is currently deposited at our core site.

The $^{230}Th_{xs}$ inventory at the shallow site GeoB6201 cannot be interpreted with confidence. A limitation is the proximity to the land, because a higher relative contribution of detrital Th to the total Th inventory is to be expected in near-shore sediments than at open ocean sites. The measured Th concentrations in these samples, however, are significantly higher than detection limits (Table 3), implying that in spite of the shallow water depth and proximity to the continent the measured $^{230}Th_{xs}$ inventory is elevated above background noise. Additional complications for calculation of Ψ arise at this particular site because of the similarity of core-top and –bottom foraminiferal radiocarbon ages, which does not allow the determination of a reliable sedimentation rate. The extracted and unextracted core-top samples yielded very different $^{230}Th_{xs0}$ concentrations, further limiting the confidence in the results. If the core-top is assumed to be modern, the focusing factor is close to unity. If either of the two core-top ages measured on foraminiferal tests is used for the determination of the sedimentation rate, strong focusing is implied. As discussed above, the core-top foraminiferal age at this site is not regarded to reflect the depositional age of the sediment.

$^{230}Th_{xs}$-normalized sediment fluxes

Normalized bulk sediment fluxes range from 0.4 to 5.8 g m^{-2} yr^{-1}, which is within the range of published values for sediments from continental margins (cf. Thomson et al., 1999).

However, sediment fluxes exhibit a very heterogeneous spatial pattern. Generally, fluxes decrease with increasing water depth (Figure 4 e). Weak correlations exist between core-top radiocarbon ages of TOC and foraminifera and $^{230}Th_{xs}$ normalized fluxes (Figure 4 a, b, c), implying that sedimentation is most strongly influenced by vertical fluxes combined with bioturbation. Bulk fluxes are more strongly correlated with water depth than TOC fluxes (Figure 4 d, e). Sites GeoB2804, GeoB2805 and GeoB2734 show the highest normalized fluxes of the entire dataset (Figure 4). These high fluxes appear to relate to the high primary productivity observed in the Brazil-Malvinas confluence zone and are reflected in higher than average sedimentary TOC contents (Figure 1b&d). These sites are also located in the area with the highest reported ΔT (Benthien & Müller, 2000), implying that in this confluence zone, a high proportion of advected particles is exported to the sea-floor. Furthermore, this area is proximal to the mouth of the Rio de la Plata, where large amounts of terrigenous materials are discharged into the ocean. Grain-size analyses have shown that this discharged sediment is relatively coarse grained, and consequently deposition occurs adjacent to the river mouth. Nevertheless, riverine input can be traced as a tongue stretching downslope to 4000 m water depth (Frenz et al., 2003) and thus likely contributes to the high fluxes and accumulation rates in the area. The discharge of terrigenous material may provide a source of ballast material enhancing export of marine organic matter by adsorption onto mineral surfaces (Hedges et al., 2001; Armstrong et al., 2002). This enhanced export may result in a high relative proportion of advected material in the sediment, if transport of the southern derived organic matter (e.g. alkenones and phytoplankton detritus) occurs in the upper water column.

Sediment flux data also shed light on the sedimentation processes at site GeoB2116, northeast of the Vema Channel. Normalized Holocene flux is very low, as is typical for deep pelagic sites. The calculated flux for the core-bottom, which has been dated at a glacial age, is significantly higher than the core-top value. This indicates that the second scenario outlined

above (slight focusing in the glacial and no sediment redistribution in the Holocene) may be more realistic for this core-site. Very low sediment flux and accumulation could thus be an alternative explanation for the "old" core-top ages at this site. More detailed down-core analyses resolving the glacial-Holocene transition would be necessary to better understand the sedimentation history at this site.

Potential transport mechanisms

In interpreting the data presented here, it is important to note that the individual proxies do not respond to the same processes. Molecular-level radiocarbon dates combined with foraminiferal ^{14}C ages can potentially elucidate the duration of differential particle transport. "Instantaneous" transport in the upper 1500 m of the water column, which would take only 7.5-30 days for average sinking velocities of 50-200 m day^{-1} (Siegel & Deuser, 1997), cannot be detected by radiocarbon analysis. In contrast, aging in intermediate reservoirs (e.g. on the shelf) followed by selective re-suspension of organic matter-rich aggregates (e.g. Ransom et al., 1998; Thomsen & Gust, 2000; Mollenhauer et al., 2003, 2005) could result in significant age offsets between the individual sediment fractions.

$^{230}Th_{xs}$ derived sediment focusing factors refer to bulk sediment and are thus not a sensitive tracer for *selective* transport of, for example, organic matter. The duration and timing of the transport process is less relevant for this proxy than the water depth in which transport occurs. As discussed in detail by François et al. (2004), only sediment redistribution by bottom nepheloid transport on a relatively flat seafloor can be accurately quantified by the $^{230}Th_{xs}$-method. Other redistribution processes, for instance through intermediate nepheloid layers or by surface currents, will result in inaccurate estimates of vertical fluxes of particles deriving from in situ production, and thus ultimately to underestimations of the degree of sediment focusing.

Consideration of all the evidence helps to constrain the modes of particle transport occurring in the Argentine Basin. Benthien & Müller (2000) suggested advection during sinking through the water column, as well as redistribution by bottom currents. The detachment of an intermediate nepheloid layer at the shelf break as described for other continental margins (e.g., Anderson et al., 1994) could supply re-suspended material from the shelf to the upper slope and deeper basins, which may or may not be pre-aged.

The alkenone radiocarbon ages suggest that long-range northward transport as inferred by Benthien & Müller (2000) does not result in significant aging of the material. This implies that the process does not involve intermediate storage of the alkenone-containing material, such as in shelf or slope sediments up-stream from our study area. Similarly, good correspondence of alkenone and foraminifera ages in sediments from the Eastern Equatorial Pacific (Mollenhauer et al., unpublished data) has been observed at a site where $^{230}Th_{xs}$ inventories imply strong focussing (Kienast et al., manuscript in preparation). Rapid northward advection of southern-derived particles is in agreement with results from Lange (1985), who observed a seasonal occurrence of subantarctic and antarctic diatom species assemblages in waters overlying the outer shelf and slope off Argentina.

However, the age differences of up to 1600 ^{14}C years between foraminifera and bulk organic matter at the sites off the mouth of the Rio de la Plata, which at the same time were identified as sites of sediment focusing, indicate that bulk organic matter experiences intermediate storage, either on land or on the shelves. Furthermore, considering the potentially high relative contribution of terrigenous organic material at this site (40-50 % according to maceral analysis; Frenz et al., 2004) together with the $^{230}Th_{xs}$ derived indication of bulk sediment focusing, redistribution of a significant fraction of the bulk sediment seems likely. Our alkenone age data suggest two scenarios: Either the intermediate storage of the marine organic matter is short-term (i.e. < 100 - 200 years, the error range of the radiocarbon ages), in which case pre-aging of a large fraction of TOC occurs on the continents; or the pre-

aged material does not contain significant amounts of alkenones. Based on these considerations, we regard a combination of advection during sinking and remobilization of primarily terrigenous material from the shelf the most likely explanation for the observed sediment characteristics. Short-duration benthic storm events associated with the eddy activity in the Brazil-Malvinas Confluence Zone are a possible mechanism for remobilization and transport. Hollister & McCave (1984), by extrapolation of their findings from the Scotian Rise, presume high abyssal eddy kinetic energy based on the observation of high surface eddy activity in this area. Similar processes have also been described for other ocean areas (e.g. Gardner & Sullivan, 1981). As outlined by Benthien & Müller (2000), transport over 100 – 1000 km during sinking is possible under the current regime prevalent in the Argentine Basin and could account for the observed temperature discrepancies, because of the existence of large temperature gradients in this region. If we assume the advection of allochthonous alkenones from waters of ambient SST of 3° C to be the sole cause for the SST discrepancies, we can calculate the proportion of alkenones deposited in margin sediments that are derived from these colder, presumably southern waters. At our margin sites, between 35 and 75 % of the total alkenones deriving from southern sources could account for the observed ΔT.

It is noteworthy that the area with largest discrepancies between alkenone-derived SSTs and measured SSTs is coincident with the highest TOC contents in surface sediments (Figure 1). Romero & Hensen (2002) furthermore report lowest relative abundance of Antarctic diatom species in this area compared to other parts of the Argentine Basin. In addition, Antarctic diatom frustules are reported to be less well preserved than those of subtropical species, indicating reworking of the sediments (Romero & Hensen, 2002). Intense reworking of the sediment is supported by the finding of elevated $^{230}Th_{xs}$ inventories, which indicate sediment focusing and re-distribution by bottom currents. Together these observations cast doubt on the notion that northward particle advection is the sole process responsible for the high ΔT values in the Brazil/Malvinas confluence zone. Instead, some of the reported

temperature discrepancy may be attributable to a non-linear temperature relationship of the $U^{K'}_{37}$ for low-temperature ocean areas (e.g. Sikes & Volkman, 1993; Conte et al., 2006).

The processes responsible for large SST discrepancies of up to -4.7 °C in the Vema Channel are most likely different from those acting on the intermediate depth continental margin off the Rio de la Plata. There the temperature anomalies are coupled with evidence for sediment winnowing, in contrast to our findings on the continental margin. With our methods we cannot detect any evidence for lateral sediment supply to these sites. Further studies will be necessary to resolve the origin of these features.

Conclusions

Our study of core-top radiocarbon ages of co-occurring foraminifera, TOC and alkenones, and $^{230}Th_{xs}$-based sediment focusing factors has helped characterize particle supply and deposition in a dynamic sedimentary environment. Comparison of core-top radiocarbon ages and sediment fluxes has shown that vertical flux is the most important factor in determining core-top ages of foraminifera and, to a certain extent, also of TOC. However, $^{230}Th_{xs}$ inventories suggest that significant sediment focusing occurs on the continental slope adjacent to the Argentine Basin, where strong discrepancies between alkenone-based sea surface temperature reconstructions and measured values have been previously reported and attributed to northward sediment transport. In contrast to other settings on continental margins (Mollenhauer et al., 2003, 2005), this focusing does not appear to result in large age offsets between foraminifera and co-occurring alkenones, despite the presumably large fraction of alkenones that are supplied by advection. Together with observations of rapid, seasonal advection of phytoplankton detritus from the south, our data set, albeit small, implies rapid supply of southern-derived particles soon after their formation, possibly as a result of transport in the upper water column. Whereas prolonged aging of particles associated with re-

suspension and downslope transport apparently dominates sedimentation in high-organic carbon continental margin settings (Mollenhauer et al., 2005), these processes seem to play a minor role on the Argentine continental margin. However, the large temperature anomalies observed in the Vema Channel cannot be attributed to sediment focusing, suggesting that several different transport processes are active. Further research will be necessary to unambiguously identify the processes governing sediment transport in the individual sedimentary environments of the Argentine Basin.

Molecular-level radiocarbon ages of marine biomarkers can help to identify post-depositional re-suspension and re-deposition. Together with sedimentological evidence for sediment transport, molecular-level radiocarbon ages can also provide information about the timing of advective processes. When used in conjunction with $^{230}Th_{xs}$-derived estimates of particle transport, sediment transport occurring in the water column and in the benthic boundary layer can be distinguished.

Acknowledgments

The crews and captains of R/V Meteor cruises M23/2, M29/1, M29/2, M46/2 and M46/3 are thanked for support during sampling. Technical support was provided by Daniel Montluçon and Li Xu (WHOI, organic geochemistry), Alan Fleer and Susan Brown-Leger (WHOI, radioisotope sample preparation and ICP/MS analysis) and by Hella Buschoff (University of Bremen, TOC and DBD analyses). The NOSAMS staff is thanked for the radiocarbon analyses. Helpful discussions with Roger François and Michiel Rutgers van der Loeff contributed substantially to the interpretation of the data. Critical comments from three anonymous reviewers helped improve this paper and are greatly appreciated. This work was funded by NSF grant # OCE-0327405 and a WHOI-NOSAMS postdoctoral scholarship to

GM, and by support from NSF and the Gary Comer Science and Education Foundation to JFM.

References

Anderson, D.M., 2001. Attenuation of millenial-scale events by bioturbation in marine sediments. Paleoceanography 16 (4), 352-357.

Anderson, R.F., Rowe, G.T., Kemp, P.F., Trumbore, S., Biscaye, P.E., 1994. Carbon budget for the mid-slope depocenter of the Middle Atlantic Bight. Deep-Sea Research II 41 (2/3), 669-703.

Antoine, D., André, J.-M., Morel, A., 1996. Oceanic primary production, 2. Estimation at global scale from satellite (coastal zone color scanner) chlorophyll. Global Biogeochemical Cycles 10 (1), 57-69.

Armstrong, R.A., Lee, C., Hedges, J.I., Honjo, S., Wakeham, S.G., 2002. A new, mechanistic model for organic carbon fluxes in the ocean based on the quantitative association of POC with ballast minerals. Deep-Sea Research II 49 219-236.

Arz H. W., Gerhardt S., Pätzold J., Röhl U., 2001. Millenial-scale changes of surface- and deep-water flow in the western tropical Atlantic linked to Northern Hemisphere high-latitude climate during the Holocene. Geology 29 (3), 239-242.

Bard, E., 2001. Paleoceanographic implications of the difference in deep-sea sediment mixing between large and fine particles. Paleoceanography 16 (3), 235-239.

Bard, E., Arnold, M., Duprat, J., Moyes, J., Duplessy, J.-C., 1987. Reconstruction of the last deglaciation: deconvolved records of $\delta^{18}O$ profiles, micropaleontological variations and accelerator mass spectrometric ^{14}C dating. Climate Dynamics 1 101-112.

Bauer, J.E., Druffel, E.R.M., Wolgast, D.M., Griffin, S., 2001. Sources and cycling of dissolved and particulate organic radiocarbon in the northwest Atlantic continental margin. Global Biogeochemical Cycles 15 (3), 615-636.

Benthien, A., Müller, P.J., 2000. Anomalously low alkenone temperatures caused by lateral particle and sediment transport in the Malvinas Current region, western Argentine Basin. Deep-Sea Research I 47 2369-2393.

Brassell, S.C., Eglinton, G., Marlowe, I.T., Pflaumann, U., Sarnthein, M., 1986. Molecular stratigraphy: A new tool for climatic assessment. Nature 320 129-133.

Broecker, W., Matsumoto, K., Clark, E., Hajdas, I., Bonani, G., 1999. Radiocarbon age differences between coexisting foraminiferal species. Paleoceanography 14 (4), 431-436.

Broecker, W.S., Klas, M., Clark, E., Bonani, G., Ivy, S., Wölfli, W., 1991. The influence of $CaCO_3$ dissolution on core top radiocarbon ages for deep-sea sediments. Paleoceanography 6 (5), 593-608.

Buscail, R., Ambatsian, P., Monaco, A., Bernat, M., 1997. ^{210}Pb, manganese and carbon: indicators of focusing processes on the northwestern Mediterranean continental margin. Marine Geology 137 271-286.

Choi, M.S., François, R., Sims, K., Bacon, M.P., Brown-Leger, S., Fleer, A.P., Ball, L., Schneider, D., Pichat, S., 2001. Rapid determination of ^{230}Th and ^{231}Pa in seawater by desolvated micro-nebulization Inductively Coupled Plasma magnetic sector mass spectrometry. Marine Chemistry 76 99-112.

Conte, M.H., Sicre, M.-A., Rühlemann, C., Weber, J.C., Schulte, S., Schulz-Bull, D., Blanz, T., 2006. Global temperature calibration of the alkenone unsaturation index ($U^{K'}_{37}$) in surface waters and comparison with surface sediments. Geochemistry, Geophysics, Geosystems 7(2), doi:10.1029/2005GC001054.

Dürkoop, A., 1998. Der Brasil-Strom im Spätquartär: Rekonstruktion der oberflächennahen Hydrographie während der letzten 400 000 Jahre. Dissertation Thesis, Department of Geosciences, University of Bremen, 121 pp.

Englebrecht, A.C., Sachs, J.P., 2005. Determination of sediment provenance at drift sites using hydrogen isotopes and unsaturation ratios in alkenones. Geochimica et Cosmochimica Acta 69(17), 4253-4265.

Fok-Pun, L., Komar, P.D., 1983. Settling velocities of planktonic foraminifera: density variations and shape effects. Journal of Foraminiferal Research 13 (1), 60-68.

François, R., Frank, M., Rutgers van der Loeff, M.M., Bacon, M.P., 2004. ^{230}Th normalization: An essential tool for interpreting sedimentary fluxes during the late Quaternary. Paleoceanography 19 doi:10.1029/2003PA000939.

Frenz, M., Höppner, R., Stuut, J.-B., Wagner, T., Henrich, R., 2003. Surface sediment bulk geochemistry and grain-size composition related to the oceanic circulation along the South American continental margin in the Southwest Atlantic. In: Wefer, G., Mulitza, S., Rathmeyer, V. (Eds.), The South Atlantic in the Late Quaternary: Reconstruction of Material Budgets and Current Systems. Springer, Berlin, Heidelberg, New York, Tokyo, pp. 347-373.

Freudenthal, T., Neuer, S., Meggers, H., Davenport, R., Wefer, G., 2001. Influence of lateral particle advection and organic matter degradation on sediment accumulation and stable nitrogen isotope ratios along a productivity gradient in the Canary Island region. Marine Geology 177 93-109.

Gardner, W.D., Sullivan, L.G., 1981. Benthic storms: temporal variability in a deep-ocean nepheloid layer. Science 213 329-331.

Guinasso, N.L., Schink, D.R., 1975. Quantitative estimates of biological mixing rates in abyssal sediments. Journal of Geophysical Research 80 (21), 3032-3043.

Hall, I.R., McCave, I.N., 1998. Glacial-interglacial variation in organic carbon burial on the slope of the N.W. European Continental Margin. Progress in Oceanography 42 37-60.

Hedges, J.I., Baldock, J.A., Gélinas, Y., Lee, C., Peterson, M., Wakeham, S.G., 2001. Evidence for non-selective preservation of organic matter in sinking marine particles. Nature 409 801-804.

Hedges, J.I., Hu, F.S., Devol, A.H., Hartnett, H.E., Tsamakis, E., Keil, R.G., 1999. Sedimentary organic matter preservation: a test for selective degradation under oxic conditions. American Journal of Science 299 529-555.

Henderson, G.M., Anderson, R.F., 2003. The U-series toolbox for paleoceanography. Reviews in Mineralogy and Geochemistry 52 493-531.

Higgins, S.M., Anderson, R.F., Marcantonio, F., Schlosser, P., Stute, M., 2002. Sediment focusing creates 100-ka cycles in interplanetary dust accumulation on the Ontong Java Plateau. Earth and Planetary Science Letters 203 383-397.

Hogg, N.G., Owens, W.B., Siedler, G., Zenk, W., 1996. Circulation in the Deep Brazil Basin. In: Wefer, G., Berger, W.H., Siedler, G., Webb, D.J. (Eds.), The South Atlantic: Present and Past Circulation. Springer, Berlin Heidelberg, pp. 249-260.

Hogg N. G., Siedler G., and Zenk W., 1999. Circulation and Variability at the Southern Boundary of the Brazil Basin. Journal of Physical Oceanography 29 (2), 145-157.

Hollister, C.D., McCave, I.N., 1984. Sedimentation under deep-sea storms. Nature 309 220-225.

Keigwin, L.D., Jones, G.A., 1994. Glacial-Holocene stratigraphy, chronology, and paleoceanographic observations on some North Atlantic sediment drifts. Deep-Sea Research 36 (6), 845-867.

Keigwin, L.D., Schlegel, M.A., 2002. Ocean ventilation and sedimentation since the glacial maximum at 3 km in the western North Atlantic. Geochemistry Geophysics Geosystems 3 doi:10.1029/2001GC000283.

Keil, R.G., Dickens, A.F., Arnarson, T., Nunn, B.L., Devol, A.H., 2004. What is the oxygen exposure time of laterally transported organic matter along the Washington margin? Marine Chemistry 92 157-165.

Lange, C.B., 1985. Spatial and seasonal variations of diatom assemblages off the Argentinian coast (South Western Atlantic). Oceanologica Acta 8 (3), 361-368.

Loubere, P., Mekik, F., François, R., Pichat, S., 2004. Export fluxes of calcite in the eastern equatorial Pacific from the Last Glacial Maximum to present. Paleoceanography 19 doi:10.1029/2003PA000986.

Lyle, M., Mitchell, N., Pisias, N.G., Mix, A., Martinez, J.I., Paytan, A., 2005. Do geochemical estimates of sediment focusing pass the sediment test in the equatorial Pacific? Paleoceanography 20 PA1005, doi:10.1029/2004PA001019.

Maamaatuaiahutapu, K., Garçon, V.C., Provost, C., Boulahdid, M., Osiroff, A.P., 1992. Brazil-Malvinas Confluence: water mass composition. Journal of Geophysical Resaerch 97 (C6), 9493-9505.

Marcantonio, F., Anderson, R.F., Higgins, S.M., Stute, M., Schlosser, P., Kubik, P.W., 2001. Sediment focusing in the central equatorial Pacific ocean. Paleoceanography 16 260-267.

Martin, W.R., Sayles, F., 2004. Organic matter cycling in sediments of the continental margin in the northwest Atlantic Ocean. Deep-Sea Research I 51 457-489.

McManus, J.F., Anderson, R.F., Broecker, W.S., Fleisher, M.Q., Higgins, S.M., 1998. Radiometrically determined sedimentary fluxes in the sub-polar North Atlantic during the last 140,000 years. Earth and Planetary Science Letters 155 29-43.

McNichol, A.P., Osborne, E.A., Gagnon, A.R., Fry, B., Jones, G.A., 1994. TIC, TOC, DIC, DOC, PIC, POC - unique aspects in the preparation of oceanographic samples for ^{14}C-AMS. Nuclear Instruments and Methods in Physics Research B 92 162-165.

Mémery, L., Arhan, M., Alvarez-Salgado, X.A., Messias, M.-J., Mercier, H., Castro, C.G., Rios, A.F., 2000. The water masses along the western boundary of the south and equatorial Atlantic. Progress in Oceanography 47 69-98.

Michaelovitch de Mahiques, M., Almeida da Silveira, I.C., de Mello e Sousa, S.H., Rodrigues, M., 2002. Post-LGM sedimentation on the outer shelf - upper slope of the northernmost part of the São Paolo Bight, southeastern Brazil. Marine Geology 181 387-400.

Milliman, J. D., Meade, R. H., 1983. Wold-wide delivery of river sediment to the oceans. Journal of Geology 91 (1) 1-21.

Mollenhauer, G., 1999. Einfluß von Bioturbation, Produktivität und Zirkulation auf ^{14}C-Datierungen an planktischen Foraminiferen. Unpublished Diplom thesis, Department of Geosciences, University of Bremen; 116 pp.

Mollenhauer, G., Eglinton, T.I., Ohkouchi, N., Schneider, R.R., Müller, P.J., Grootes, P.M., Rullkötter, J., 2003. Asynchronous alkenone and foraminifera records from the Benguela Upwelling System. Geochimica et Cosmochimica Acta 67 (12), 2157-2171.

Mollenhauer, G., Kienast, M., Lamy, F., Meggers, H., Schneider, R.R., Hayes, J.M., Eglinton, T.I., 2005. An evaluation of ^{14}C age relationships between co-occurring foraminifera, alkenones, and total organic carbon in continental margin sediments. Paleoceanography 20 PA1016; doi:10.1029/2004PA001103.

Mollenhauer, G., Schneider, R.R., Jennerjahn, T.C., Müller, P.J., Wefer, G., 2004. Organic carbon accumulation in the South Atlantic Ocean: its modern, mid-Holocene and last glacial distribution. Global and Planetary Change 40 249-266.

Müller, P.J., Kirst, G., Ruhland, G., von Storch, I., Rosell-Melé, A., 1998. Calibration of the alkenone paleotemperature index $U^{K'}_{37}$ based on core tops from the eastern South Atlantic and the global ocean. Geochimica et Cosmochimica Acta 62 (10), 1757-1772.

Ohkouchi, N., Eglinton, T.I., Keigwin, L.D., Hayes, J.M., 2002. Spatial and temporal offsets between proxy records in a sediment drift. Science 298 1224-1227.

Ohkouchi, N., Xu, L., Reddy, C.M., Montluçon, D., Eglinton, T.I., 2004. Radiocarbon dating of alkenones from marine sediments: I. Isolation protocol. Radiocarbon 47 425-432.

Olson, D.B., Podestá, G.P., Evans, R.H., Brown, O.B., 1988. Temporal variations in the separation of Brazil and Malvinas Currents. Deep-Sea Research 35 (12), 1971-1990.

Paytan, A., Kastner, M., Chavez, F., 1996. Glacial to interglacial fluctuations in productivity in the equatorial Pacific as indicated by marine barite. Science 214 1355-1357.

Pearson, A., McNichol, A., Schneider, R.J., von Reden, K.F., Zheng , Y., 1998. Microscale AMS ^{14}C measurement at NOSAMS. Radiocarbon 40 (1), 61-75.

Peterson, R.G., 1992. The boundary currents in the western Argentine Basin. Deep-Sea Research 39 (3/4), 623-644.

Peterson, R.G., Johnson, C.S., Krauss, W., Davis, R.E., 1996. Lagrangian Measurements in the Malvinas Current.
In: Wefer, G., Berger, W.H., Siedler, G., Webb, D.J. (Eds.), The South Atlantic: Present and Past Circulation. Springer, Berlin Heidelberg, pp. 239-247.

Peterson, R.G., Stramma, L., 1991. Upper-level circulation in the South Atlantic Ocean. Progress in Oceanography 26 1-73.

Piola, A.R., Bianchi, A.A., Rivas, A.L., Palma, E.D., Matano, R.P., Bleck, R., 2001. The Brazil-Malvinas confluence. Online poster.
http://www.po.gso.uri.edu/wbc/Piola/bmc.htm.

Prahl, F.G., Muehlhausen, L.A., Zahnle, D.L., 1988. Further evaluation of long-chain alkenones as indicators of paleoceanographic conditions. Geochimica et Cosmochimica Acta 62 (1), 69-77.

Ransom, B., Shea, K.F., Burkett, P.J., Bennett, R.H., Baerwald, R., 1998. Comparison of pelagic and nepheloid layer marine snow: implicatons for carbon cycling. Marine Geology 150 39-50.

Reid, J.L., Nowlin Jr., W.E., Patzert, W.C., 1977. On the characteristics and circulation of the Southwestern Atlantic Ocean. Journal of Physical Oceanography 7 62-91.

Romero, O., Hensen, C., 2002. Oceanographic control of biogenic opal and diatoms in surface sediments of the Southwestern Atlantic. Marine Geology 186 (3-4), 263-280.

Sanchez-Cabeza, J.A., Masqué, P., Ani-Ragolta, I., Merino, J., Frignani, M., Alvisi, F., Palanques, A., Puig, P., 1999. Sediment accumulation rates in the southern Barcelona continental margin (NW Mediterranean Sea) derived from ^{210}Pb and ^{137}Cs chronology. Progress in Oceanography 44 313-332.

Santschi, P.H., Guo, L., Walsh, I.D., Quigley, M.S., Baskaran, M., 1999. Boundary exchange and scavenging of radionuclides in continental margin waters of the Middle Atlantic Bight: implications for organic carbon fluxes. Continental Shelf Research 19 (5), 609-636.

Schlünz, B., Schneider, R.R., Müller, P.J., Showers, W.J., Wefer, G., 1999. Terrestrial organic carbon accumulation on the Amazonas deep sea fan during the last glacial sea level low stand. Chemical Geology 159 263-281.

Schwarz, B., Mangini, A., Segl, M., 1996. Geochemistry of a piston core from Ontong Java Plateau (western equatorial Pacific): evidence for sediment redistribution and changes in paleoproductivity. Geologische Rundschau 85 536-545.

Seiter, K., Hensen, C., Schröter, J., Zabel, M., 2004. Organic carbon content in surface sediments - defining regional provinces. Deep-Sea Research I 51 2001-2026.

Siegel, D.A., Deuser, W.G., 1997. Trajectories of sinking particles in the Sargasso Sea: modeling of statistical funnels above deep-ocean sediment traps. Deep-Sea Research I 44 (9-10), 1519-1541.

Sikes, E.L., Volkman, J.K., 1993. Calibration of alkenone unsaturation ratios ($U^{K'}_{37}$) for paleotemperature estimation in cold polar waters. Geochimica et Cosmochimica Acta 59 3009-3107.

Stuiver, M., Polach, H.A., 1977. Discussion, Reporting of ^{14}C data. Radiocarbon 19 (3), 355-363.

Stuiver, M., Reimer, P., 2005. CALIB 5.0, online calibration software, http://radiocarbon.pa.qub.ac.uk/calib/.

Suman, D.O., Bacon, M.P., 1989. Variations in Holocene sedimentation in the North Atlantic basin determined from ^{230}Th measurements. Deep-Sea Research 36 869-878.

Thomsen, L., Gust, G., 2000. Sediment erosion thresholds and characteristics of resuspended aggregates on the western European continental margin. Deep-Sea Research I 47 1881-1897.

Thomsen, L., van Weering, T.C.E., 1998. Spatial and temporal variability of particulate matter in the benthic boundary layer at the N. W. European Continental Margin (Goban Spur). Progress in Oceanography 42 61-76.

Thomson, J., Colley, S., Anderson, R., Cook, G.T., MacKenzie, A.B., 1995. A comparison of sediment accumulation chronologies by the radiocarbon and $^{230}Th_{excess}$ methods. Earth and Planetary Science Letters 133 59-70.

Thomson, J., Nixon, S., Summerhayes, C.P., Schönfeld, J., Zahn, R., Grootes, P.M., 1999. Implications for sedimentation changes on the Iberian margin over the last two glacial/interglacial transitions from $(^{230}Th_{excess})_0$ systematics. Earth and Planetary Science Letters 165 255-270.

Figure captions

Figure 1: Maps of the study area: a) bathymetry and major bathymetric features (map generated by OMC – online map creator), contour interval is 500 m; b) annual mean phytoplankton pigment concentrations as determined by satellite imagery (CZCS Nov. 1978 – June 1986) and surface currents; BMC indicates the Brazil-Malvinas Confluence; c) core sites analysed in this study (triangles) plotted on the contour map of differences between alkenone-based sea surface temperature estimates and measured values (ΔT); sites on which contour map is based are given as open circles (modified after Benthien & Müller, 2000), underlined core numbers indicate sites for which alkenone core-top radiocarbon ages have been obtained; d) core-top sediment TOC content in % dry weight; core sites used for map interpolation are given as open circles (modified after Mollenhauer et al., 2004).

Figure 2: Core-top radiocarbon ages of planktic foraminifera (circles), alkenones (diamonds), and TOC (squares). Ages are given in conventional radiocarbon ages in years BP (Stuiver & Polach, 1977); error bars denote 1 σ errors. Contour lines on map are ΔT from Benthien & Müller (2000).

Figure 3: Study sites and data projected on a plane defined by latitude and water depth of the sites. a) Schematic representation of water masses and flow directions in the study area (MC: Malvinas Current; BC: Brazil Current; UCDW and LCDW: Upper and Lower Circumpolar Deepwater, respectively; NADW: North Atlantic Deep Water; AABW: Antarctic Bottom Water). b) Study site locations projected on the plane. c) Core-top TOC (italics, left) and foraminiferal (right) radiocarbon ages in ^{14}C years BP. Open symbols represent foraminiferal data from the literature (Table 4). d) Differences between reconstructed and measured SST (from Benthien & Müller, 2000 and from this study). e) $^{230}Th_{xs}$ derived sediment focusing factors Ψ.

Figure 4: ^{230}Th normalized bulk sediment and TOC fluxes plotted versus core-top ages (A, B, C), water depth (D, E), and age difference between TOC and foraminifera in core-tops (F). The individual core sites are identified by lower case letters (Brazil Basin: a) GeoB2124, b) GeoB2116, c) GeoB6201; Vema Channel: d) GeoB2826, d) GeoB2824; Argentine Basin: f) GeoB2804, g) GeoB2805, h) GeoB2734, i) GeoB2728, k) GeoB6339).

Figure

Click here to download Figure: Mollenhauer et al Figure 1.eps

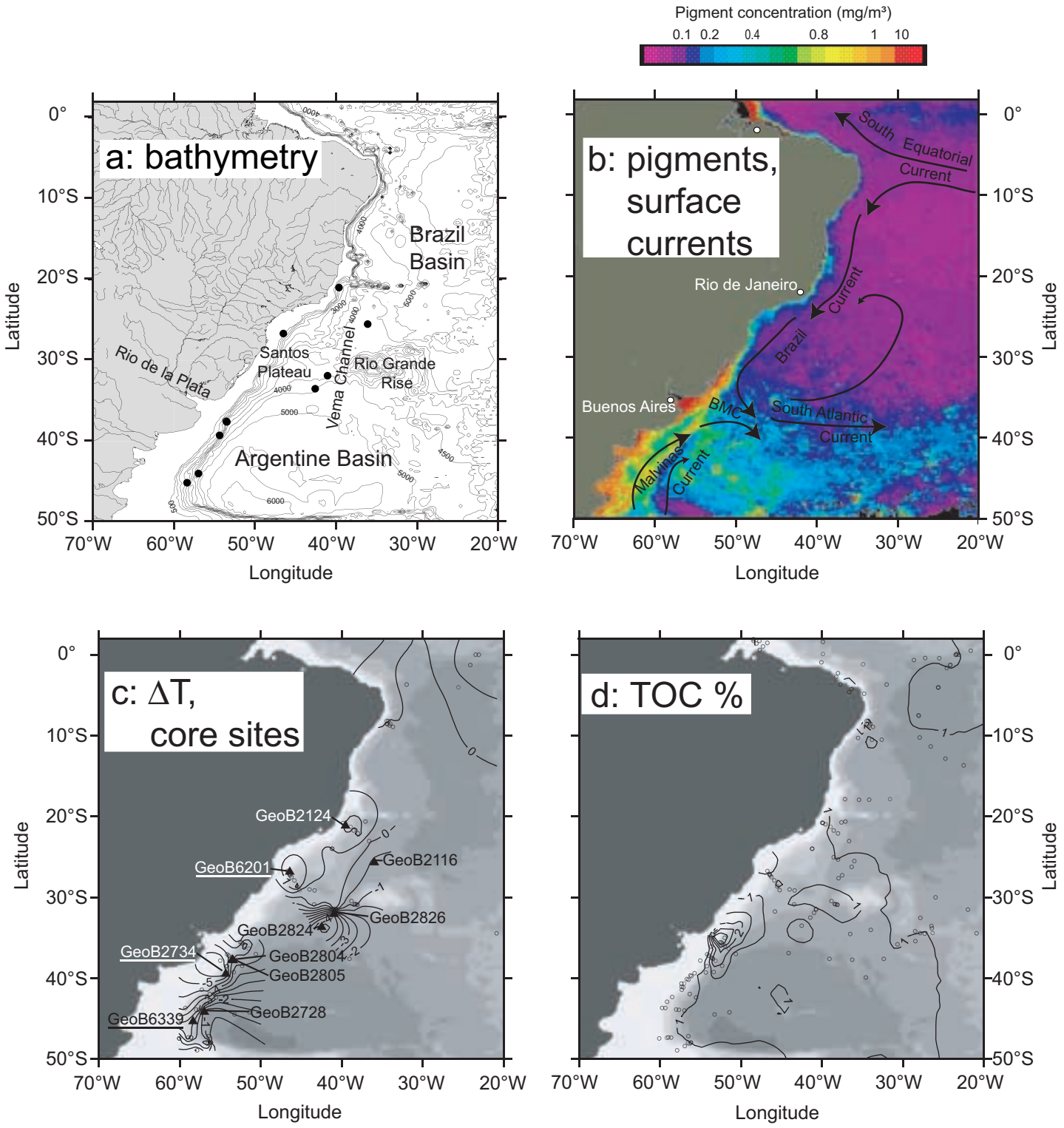

Mollenhauer et al., Figure 1

Figure

Click here to download Figure: Mollenhauer et al Figure2.eps

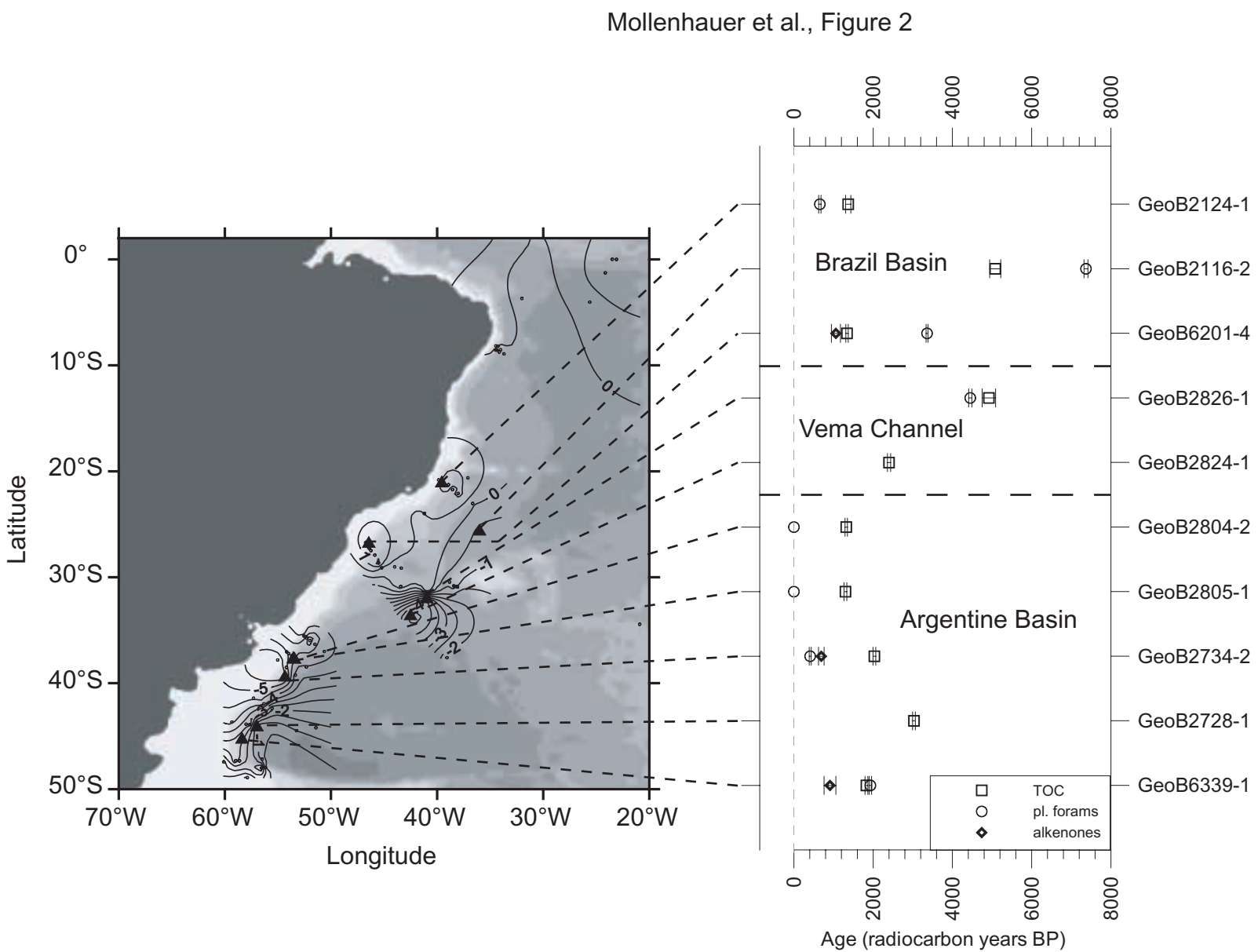

Figure

Click here to download Figure: Mollenhauer et al Figure3.eps

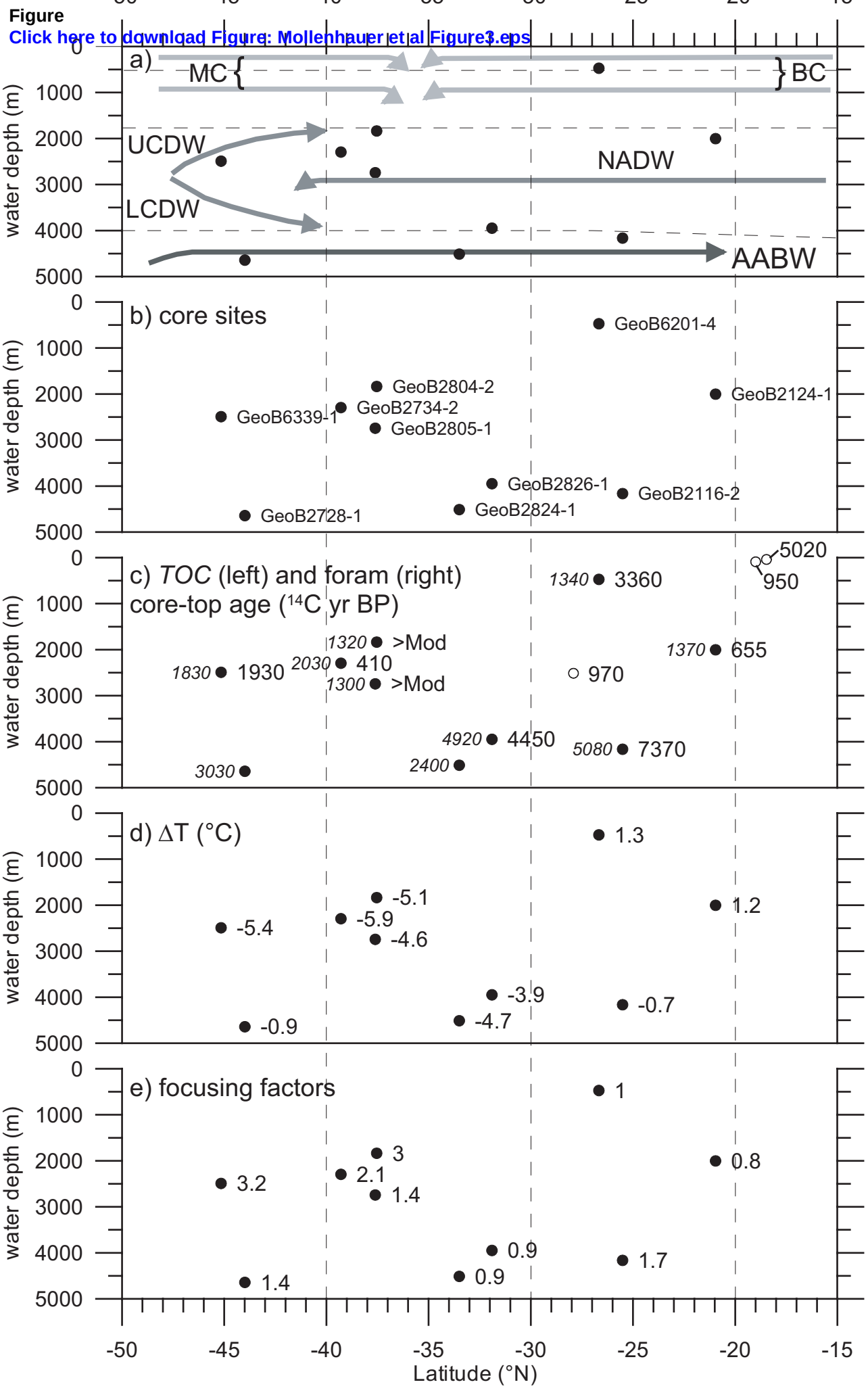

Mollenhauer et al., Figure 3

Figure

Click here to download Figure: Mollenhauer et al Figure4.eps

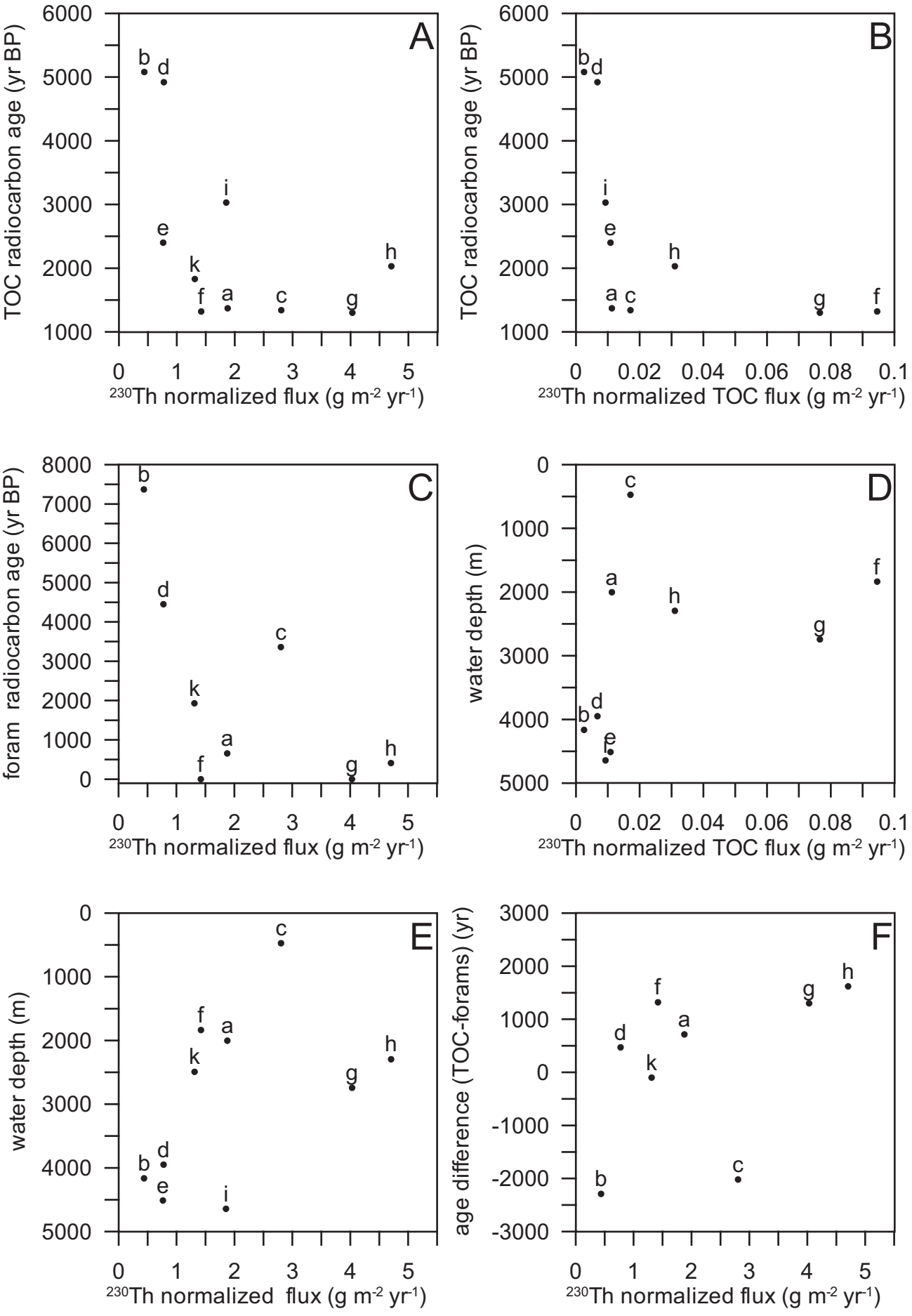

Mollenhauer et al., Figure 4

Table

Click here to download Table: Mollenhauer et al_Table1.doc

Table 1: Core locations

Sample	Latitude (°N)	Longitude (°E)	Water depth (m)
GeoB2124-1	-20.96	-39.56	2003
GeoB2116-2	-25.51	-36.00	4164
GeoB6201-4	-26.67	-46.44	473
GeoB2826-1	-31.90	-40.97	3949
GeoB2824-1	-33.50	-42.50	4512
GeoB2804-2	-37.54	-53.54	1836
GeoB2805-1	-37.61	-53.44	2743
GeoB2734-3	-39.29	-54.34	2295
GeoB2728-1	-43.99	-56.97	4643
GeoB6339-1	-45.15	-58.38	2492

Table

Click here to download Table: Mollenhauer et al_Table2.doc

Sample	Foraminifera				TOC		Alkenones		
	species	Depth [cm]	^{14}C age [yr BP]	Calibrated calendar age [yr BP]	Depth [cm]	^{14}C age [yr BP]	Depth [cm]	^{14}C age [yr BP]	ΔT [°C]
GeoB2124-1	*G. ruber pink*	0-1	655±30	290	0-2	1370±65			1.2
	G. ruber pink	30-31	11000±65	12650					
GeoB2116-2	*mixed planktics*	0-1	7370±50	7840	0-1	5080±140			-0.7
	G. sacculifer	39-40	16750±120	19500					
GeoB6201-4	*G. ruber*	0-1	3360±25	3240	0-1	1340±30	0-2	1060±115	*1.3*
	G. ruber	0-1	3240±35	3060					
	G. ruber	10-11	3660±30	3570					
GeoB2826-1	*mixed planktics*	0-1	4450±40	4630	0-2	4920±170			-3.9
	mixed planktics	7-8	8660±40	9340					
GeoB2824-1					0-2	2400±40			-4.7
GeoB2804-2	*mixed planktics*	0-1	modern	0	1-2	1320±30			-5.1
	mixed planktics	11-12	1230±30	770					
GeoB2805-1	*G. inflata*	0-1	modern	0	0-1	1300±35			-4.6
	G. inflata	10-11	1480±30	1020					
GeoB2734-3	*G. bulloides*	0-2	410±25	40	0-2	2030±35	0-2	690±70	-5.9
	G. bulloides	10-11	1240±30	780					
GeoB2728-1					0-1	3030±35			-0.9
GeoB6339-1	*G. bulloides*	0-1	1930±30	1480	0-1	1830±35	0-2	910±150	*-5.4*
	G. bulloides	20-21	5000±35	5360					

Table 2: Core-top radiocarbon ages of planktic foraminifera, TOC and alkenones, and deviations of alkenone-based reconstructed sea-surface temperatures from measured values (ΔT). No foraminiferal ages could be obtained for cores below 4000 m water depth due to calcite dissolution; alkenone ages are corrected for a constant blank contribution of 0.08 ± 0.02 µmol C assuming a radiocarbon concentration of blank C of 0.25 fMC. ΔT values are from Benthien & Müller (2000), except those printed in italics, which are based on alkenone SST estimates from this study.

Table

Click here to download Table: Mollenhauer et al_Table3.doc

sample	sample depth	age	water depth	DBD	TOC	^{230}Th	^{238}U	$^{230}Th_{xs}$	$^{230}Th_{xs0}$	focusing factor Ψ			Flux		
								R=0.6	R=0.6		Error			Error	
	[cm]	[kyr]	[m]	[g/cm³]	[wt. %]	[dpm/g]	[dpm/g]	[dpm/g]	[dpm/g]		+	-	[g/m²yr]	+	-
GeoB2124 extracted	0-1			0.26		4.25	1.05	**3.30**	**3.34**	*0.8*					
GeoB2124	0-1	0.29	2003	0.26	0.6	3.74	1.01	**2.84**	**2.85**	**0.8**	0.1	0.1	**1.9**	0.1	0.1
GeoB2124	30-31	12.65		*0.7*		5.17	1.68	**3.21**	**3.64**				**1.5**	0.2	0.1
GeoB2116	0-1	7.82	4164	0.19	0.6	25.09	1.22	**23.63**	**25.41**	**1.7**	0.0	0.0	**0.4**	0.0	0.0
GeoB2116	39-40	19.50		*0.7*		8.79	1.31	**7.31**	**8.78**				**1.3**	0.0	0.0
GeoB6201 extracted	0-1	3.06; 3.24	473	*0.6*		1.75	1.19	**0.77**	**0.79**	***0.9 - 1.1***			**1.6**	0.5	0.2
GeoB6201	0-1	*0;*		*0.6*	0.6	1.78	1.27	**0.45**	**0.45**	***(6.7, 10.3)***			**2.8**	2.7	0.9
GeoB6201	10-11	3.57		*0.7*		1.72	1.25	**0.76**	**0.78**				**1.6**	0.4	0.3
GeoB2826	0-2	4.63	3949	0.26	0.9	14.18	1.18	**13.04**	**13.60**	**0.9**	0.0	0.0	**0.8**	0.0	0.0
GeoB2826	7-8	9.34		*0.7*		13.74	1.18	**12.53**	**13.65**				**0.8**	0.0	0.0
GeoB2824	0-2	*2*	4512	0.16	1.4	16.61	1.31	**15.49**	**15.77**	**0.9**	0.0	0.0	**0.8**	0.0	0.0
GeoB2824	10-11	*8.5*		*0.7*		16.97	1.43	**15.78**	**17.12**				**0.7**	0.0	0.0
GeoB2804	1-2	0	1836	0.49*	1.6*	4.21	1.05	**3.45**	**3.45**	**3.0**	0.2	0.2	**1.4**	0.1	0.1
GeoB2804	11-12	0.77		*0.7*		1.67	1.54	**0.85**	**0.85**				**5.8**	1.1	0.8
GeoB2805	0-1	0	2743	0.41	1.9	2.72	1.09	**1.82**	**1.82**	**1.4**	0.1	0.1	**4.0**	0.4	0.3
GeoB2805	9-10	1.015		*0.7*		3.00	2.21	**2.16**	**2.17**				**3.4**	0.2	0.2
GeoB2734 extracted	0-2			0.76		1.81	0.83	**1.16**	**1.16**	*2.1*					
GeoB2734	0-2	0	2295	0.76	0.7	1.96	0.88	**1.30**	**1.30**	**2.1**	0.2	0.2	**4.7**	0.4	0.4
GeoB2734	10-11	0.78		*0.9*		1.92	1.39	**1.29**	**1.29**				**4.7**	0.4	0.4
GeoB2728	0-1	*2*	4643	0.59	0.5	7.18	0.84	**6.57**	**6.69**	**1.4**	0.0	0.0	**1.9**	0.0	0.0
GeoB2728	8-9	*4.7*		*0.7*		11.08	1.32	**9.95**	**10.60**				**1.2**	0.0	0.0
GeoB6339 extracted	0-1	1.48		*0.7*		5.53	0.55	**5.15**	**5.21**	*3.2*			**1.3**	0.0	0.0
GeoB6339	0-1		2492	*0.7*	n.d.	5.36	0.53	**5.01**	**5.08**	**3.2**	0.0	0.0	**1.3**	0.0	0.0
GeoB6339	20-21	5.36		*0.9*		5.58	2.50	**5.13**	**5.28**				**1.3**	0.0	0.0

Table 3: ICP-MS measurements of uranium series isotopes in sediments, calculated focusing factors Ψ and fluxes. For core-tops of GeoB2124, GeoB6201, GeoB2734 and GeoB6339, U series measurements were made on original and on solvent-extracted sediment material. Good agreement between both values is achieved for GeoB2124, GeoB2734 and GeoB6339. Calculations are based on calibrated radiocarbon ages of foraminifera or assumed ages (printed in italic font). Dry bulk densities (DBD) are measured values (normal font) and assumed values (italic). Assumptions are based on comparison with data from nearby cores (see text). For the calculation of $^{230}Th_{xs}$ and $^{230}Th_{xs0}$ (decay corrected), an average Atlantic Ocean $^{238}U/^{232}Th$ ratio of R=0.6 was assumed (McManus et al., 1998). Errors given for focusing factor and flux estimates are based on R=0.6 ± 0.1. Errors associated with the uncertainties of sedimentation rates are larger (see text). Focusing factors are based on mean $^{230}Th_{xs0}$ of core-top and -bottom

sediments. Ψ printed in italic font are based on mean surface sediment values (extracted and unextracted sediment material). The wide range of Ψ calculated for GeoB6201, a very shallow core, reflects uncertainties in the age model. Low values of approximately 1 (italic and underlined) are obtained when assuming a core-top age of 0 and taking averages of 2 or 3 measured $^{230}Th_{xs0}$. Ψ of 6.6 and 10.3 are calculated when using the measured core-top ages of 3.06 and 3.24 kyr, respectively. *determined for 0-1 cm

Table
Click here to download Table: Table 4.doc

Table 4: Locations and published radiocarbon ages of carbonate sediment fractions.

Station	Latitude (°N)	Longitude (°E)	water depth (m)	conv. radiocarbon age (^{14}C yr BP)	planktic foraminiferal species / dated matieral	Reference
GeoB2109-3	-27.91	-45.87	2513	970±30	*N. dutertrei*	Mollenhauer (1999)
GeoB2204-1	-8.53	-34.02	2080	2050±20	*G. sacculifer*	Dürkoop (1998)
GeoB3230-1	-19.00	-38.46	90	950±50	bivalves, gastropods, byrozoans	J. Pätzold, H. Arz, unpublished
GeoB3232-2	-18.47	-39.03	40	5020±60	bivalves	J. Pätzold, H. Arz, unpublished
GeoB3910-3	-4.25	-36.35	2361	565±30	*G. sacculifer*	Arz et al., 2001